

Accepted Manuscript

Short communication

A mathematical analysis to address the 6 degree-of-freedom segmental power imbalance

Anahid Ebrahimi, John D. Collins, Thomas M. Kepple, Kota Z. Takahashi, Jill S. Higginson, Steven J. Stanhope

PII: S0021-9290(17)30574-2

DOI: <https://doi.org/10.1016/j.jbiomech.2017.10.034>

Reference: BM 8436

To appear in: *Journal of Biomechanics*

Accepted Date: 28 October 2017



Please cite this article as: A. Ebrahimi, J.D. Collins, T.M. Kepple, K.Z. Takahashi, J.S. Higginson, S.J. Stanhope, A mathematical analysis to address the 6 degree-of-freedom segmental power imbalance, *Journal of Biomechanics* (2017), doi: <https://doi.org/10.1016/j.jbiomech.2017.10.034>

This is a PDF file of an unedited manuscript that has been accepted for publication. As a service to our customers we are providing this early version of the manuscript. The manuscript will undergo copyediting, typesetting, and review of the resulting proof before it is published in its final form. Please note that during the production process errors may be discovered which could affect the content, and all legal disclaimers that apply to the journal pertain.

A mathematical analysis to address the 6 degree-of-freedom segmental power imbalance

Anahid Ebrahimi, BS¹; John D. Collins, MA^{2,3}; Thomas M. Kepple, MS⁴; Kota Z. Takahashi, PhD⁵; Jill S. Higginson, PhD^{1,3,6}; Steven J. Stanhope, PhD^{1,3,6,7}

¹Department of Mechanical Engineering, University of Delaware, Newark, DE, USA

²Naval Medical Center, San Diego, CA, USA

³Biomechanics and Movement Science Interdisciplinary Program, University of Delaware, Newark, DE, USA

⁴C-motion, Inc., Germantown, MD, USA

⁵Department of Biomechanics, University of Nebraska at Omaha, Omaha, NE, USA

⁶Department of Biomedical Engineering, University of Delaware, Newark, DE, USA

⁷Department of Kinesiology and Applied Physiology, University of Delaware, Newark, DE, USA

For submission to the *Journal of Biomechanics* as a Short Communication

KEY WORDS: rate of energy change; kinetic method; kinematic method; gait analysis

WORD COUNT (Intro to Disc): 2,148 of 2,000

Corresponding author:

Anahid Ebrahimi, BS
University of Delaware
540 South College Ave
STAR Campus - Room 201
Newark, DE 19713
Phone: (530) 574-7601
E-mail: anahide@udel.edu

ABSTRACT (WORD COUNT: 250 of 250)

Segmental power is used in human movement analyses to indicate the source and net rate of energy transfer between the rigid bodies of biomechanical models. Segmental power calculations are performed using segment endpoint dynamics (kinetic method). A theoretically equivalent method is to measure the rate of change in a segment's mechanical energy state (kinematic method). However, these two methods have not produced experimentally equivalent results for segments proximal to the foot, with the difference in methods deemed the "power imbalance." In a 6 degree-of-freedom model, segments move independently, resulting in relative segment endpoint displacement and non-equivalent segment endpoint velocities at a joint. In the kinetic method, a segment's distal end translational velocity may be defined either at the anatomical end of the segment or at the location of the joint center (defined here as the proximal end of the adjacent distal segment). Our mathematical derivations revealed the power imbalance between the kinetic method using the anatomical definition and the kinematic method can be explained by power due to relative segment endpoint displacement. In this study, we tested this analytical prediction through experimental gait data from nine healthy subjects walking at a typical speed. The average absolute segmental power imbalance was reduced from 0.023 - 0.046 W/kg using the anatomical definition to ≤ 0.001 W/kg using the joint center definition in the kinetic method (95.56 – 98.39% reduction). Power due to relative segment endpoint displacement in segmental power analyses is substantial and should be considered in analyzing energetic flow into and between segments.

INTRODUCTION

A segmental power analysis is a useful biomechanical tool (Caldwell and Forrester, 1992), which has been used in analyzing human movement to indicate the source and net rate of energy transfer (flow) between the rigid bodies of biomechanical models (Aleshinsky, 1986; Robertson and Winter, 1980; van Ingen Schenau and Cavanagh, 1999). Segmental power calculations utilize segment endpoint dynamics (kinetic method), but a theoretically equivalent method is to measure changes in the segment's energy state (kinematic method) (Zajac et al., 2002). Several researchers have used independent measures of segmental power to explain how power flow between segments relates to changes in the energy state of the segments in activities like walking (Aleshinsky, 1986; Caldwell and Forrester, 1992; Robertson and Winter, 1980; Zelik et al., 2015), pedaling (Kautz et al., 1994; Kautz and Neptune, 2002), running (Caldwell and Forrester, 1992), wheelchair propulsion (Guo et al., 2003), lifting (De Looze et al., 1992), and various endurance sports (van Ingen Schenau and Cavanagh, 1999). Researchers have also used this mathematical equivalence to assess the accuracy of specific models (McGibbon and Krebs, 1998) based on how closely powers calculated using the kinetic method match with those using the kinematic method. Several investigators theorized the kinematic method is more accurate as it is based only on motion and anthropometric estimates (Caldwell and Forrester, 1992; Robertson and Winter, 1980).

The models and corresponding model assumptions used to analyze segmental power flow influence how results may be interpreted. A pin-joint model, which fixes segment ends at a coincident point, has been used for two- (i.e. sagittal plane) or three-dimensional gait analyses (De Looze et al., 1992; McGibbon and Krebs, 1998; Robertson and Winter, 1980). However, use of the pin-joint model may require segment lengths and inertial alignment (e.g. segment center of

mass position) to change due to a shared joint center with adjacent segments, thus violating rigid body assumptions. Conversely, a 6 degree-of-freedom (6 DOF) model for three-dimensional gait analyses fixes segment characteristics, which can lead to relative displacement between adjacent segment ends, and thus non-equivalent segment endpoint velocities at a joint (Buczek et al., 1994; McGibbon and Krebs, 1998). While both models have limitations, the translational power resulting from the intersegmental joint force and the segment endpoint velocities in a 6 DOF model is valuable to include for a complete mechanical energy analysis of human gait (Buczek et al., 1994; Geil et al., 2000; Zelik et al., 2015).

Independent of chosen model, the kinetic and kinematic methods typically do not provide experimentally equivalent results, leading to a “power imbalance” (PI) (McGibbon and Krebs, 1998). Using a three-dimensional analysis, McGibbon and Krebs reported using the pin-joint model resulted in a mean absolute PI over stance ranging from 9.9 – 25.6 W for the shank and 6.8 – 23.4 W for the thigh. The mean absolute PI was reduced when segment lengths were fixed and radial velocities of the distal and proximal ends of the segment relative to the segment’s center of mass were accounted for (1.1 – 5.0 W and 0.7 – 4.1 W for the shank and thigh, respectively). However, while fixed segment lengths reduced the PI within a segment, there was a large power discrepancy between segment ends across a joint (e.g. 10.7 – 37.8 W at the knee), which was considered an “energy well” (McGibbon and Krebs, 1998).

Thus, identifying the source of the PI is important for effectively characterizing energetic measures in the study of human movement. To date, the foot is the only segment whose PI was computationally accounted for by the inclusion of a calculation for distal foot segmental power (Siegel et al., 1996).

The purpose of this study was to determine the source of PI by conducting a mathematical analysis to equate the kinematic and kinetic methods for a 6 DOF model. We theorized accounting for power due to relative displacement between the distal end of a segment and the joint center in the kinetic model (relative displacement power) would reduce the PI. We then experimentally characterized the PI with and without accounting for the relative displacement power.

COMPUTATIONAL DEVELOPMENT

Using Newton-Euler formulas (Siegler and Liu, 1997) in inverse dynamics calculations (Robertson et al., 2013), the general form for the proximal joint intersegmental force ($\vec{F}_{p,m}$) for any segment m , linked by n number of segments, is given by equation 1 where m_m , \vec{a}_m , \vec{g} , and \vec{F}_{grf} represent the segment mass, segment center of mass acceleration, gravity (9.81 m/s^2), and ground reaction force, respectively. Similarly, the proximal net joint moment ($\vec{M}_{p,m}$) is given by equation 2 where I_m , \vec{a}_m , $\vec{\omega}_m$, and $\vec{\tau}_{free}$ represent the moment of inertia, angular acceleration, angular velocity, and free moment, respectively. The $\vec{r}_{COM,n/m}$ and $\vec{r}_{COP,m}$ are vectors from the proximal end of the m^{th} segment end to the center of mass of the n^{th} segment and to the center of pressure, respectively (Fig. 1).

$$\vec{F}_{p,m} = [\sum_{n=1}^m (m_n \vec{a}_n - m_n \vec{g})] - \vec{F}_{grf} \quad (1)$$

$$\vec{M}_{p,m} = [\sum_{n=1}^m (I_n \vec{a}_n + \vec{\omega}_n \times I_n \vec{\omega}_n + \vec{r}_{COM,n/m} \times (m_n \vec{a}_n - m_n \vec{g}))] - \vec{\tau}_{free} - \vec{r}_{COP,m} \times \vec{F}_{grf} \quad (2)$$

The proximal segment translational velocity is given by equation 3 where $\vec{r}_{p,m}$ is the vector from the center of mass to the proximal (p) end of the segment, and the segment velocity is represented by \vec{v}_m .

$$\vec{v}_{p,m} = \vec{v}_m + \vec{\omega}_m \times \vec{r}_{p,m} \quad (3)$$

In an anatomically relevant (AR) definition, distal translational velocity is given by equation 4 where $\vec{r}_{d-AR,m}$ is the vector from the center of mass to the distal (d) end of the segment.

$$\vec{v}_{d-AR,m} = \vec{v}_m + \vec{\omega}_m \times \vec{r}_{d-AR,m} \quad (4)$$

However, the AR definition of distal velocity is not always coincident with the point of force application (i.e. the joint center), which is defined here as the proximal end of the adjacent distal segment (Fig. 1). Therefore, there exists a displacement vector ($\vec{r}_{m/m-1}$) between the distal end of segment m and proximal end of segment $m-1$ with a velocity given by equation 5.

$$\vec{v}_{m/m-1} = \vec{\omega}_m \times \vec{r}_{m/m-1} \quad (5)$$

In a joint center (JC) definition, distal translational velocity is given by equation 6 where $\vec{r}_{d-JC,m}$ is the vector from the center of mass to the joint center. This vector is equivalent to the sum of $\vec{r}_{d-AR,m}$ and $\vec{r}_{m/m-1}$ (Fig. 1).

$$\vec{v}_{d-JC,m} = \vec{v}_m + \vec{\omega}_m \times \vec{r}_{d-JC,m} = \vec{v}_m + \vec{\omega}_m \times (\vec{r}_{d-AR,m} + \vec{r}_{m/m-1}) \quad (6)$$

Segmental power using the kinetic method can be calculated using the AR definition ($P_{AR,m}$) in equation 7, where distal joint intersegmental force and net joint moment are represented by $\vec{F}_{d,m}$ and $\vec{M}_{d,m}$, respectively. The pelvis segment ($m = 4$) is calculated using proximal powers as well as left and right $\vec{F}_{d,4}$ and $\vec{M}_{d,4}$. The $\vec{r}_{d-AR,4}$ is from the center of mass to the left or right hip joint center positions in the pelvis coordinate system (as defined in the static model pose).

$$P_{AR,m} = \vec{M}_{p,m} \cdot \vec{\omega}_m + \vec{M}_{d,m} \cdot \vec{\omega}_m + \vec{F}_{p,m} \cdot \vec{v}_{p,m} + \vec{F}_{d,m} \cdot \vec{v}_{d-AR,m} \quad (7)$$

Segmental power calculated using the JC definition ($P_{JC,m}$) can be represented using equations 6 and 7 as shown in equation 8a. The power due to the displacement between segment ends of adjacent segments, or relative displacement power ($P_{m/m-1}$), is shown in equation 8b.

$$P_{JC,m} = \vec{M}_{p,m} \cdot \vec{\omega}_m + \vec{M}_{d,m} \cdot \vec{\omega}_m + \vec{F}_{p,m} \cdot \vec{v}_{p,m} + \vec{F}_{d,m} \cdot \vec{v}_{d-JC,m} = P_{AR,m} + P_{m/m-1} \quad (8a)$$

Where

$$P_{m/m-1} = \vec{F}_{d,m} \cdot \vec{v}_{m/m-1} \quad (8b)$$

Equations 1- 3 and 6 can be substituted into equation 8a to achieve equation 9 (see Appendix for complete details).

$$\begin{aligned} P_{JC,m} &= \vec{M}_{p,m} \cdot \vec{\omega}_m + \vec{M}_{d,m} \cdot \vec{\omega}_m + \vec{F}_{p,m} \cdot \vec{v}_{p,m} + \vec{F}_{d,m} \cdot \vec{v}_{d-JC,m} \\ &= (I_m \vec{\alpha}_m + \vec{\omega}_m \times I_m \vec{\omega}_m) \cdot \vec{\omega}_m + (m_m \vec{a}_m - m_m \vec{g}) \cdot \vec{v}_m - (\vec{r}_{COP,m} \times \vec{F}_{grf}) \cdot \vec{\omega}_m + \\ &\quad (\vec{r}_{COP,m-1} \times \vec{F}_{grf}) \cdot \vec{\omega}_m - \vec{F}_{grf} \cdot (\vec{\omega}_m \times \vec{r}_{p,m}) + \vec{F}_{grf} \cdot (\vec{\omega}_m \times \vec{r}_{d-AR,m}) + \vec{F}_{grf} \cdot (\vec{\omega}_m \times \\ &\quad \vec{r}_{m/m-1}) \quad (9) \end{aligned}$$

The rate of energy change ($\frac{d}{dt} E_m$) using the kinematic method is calculated in equation 10, which sums the rotational kinetic, translational kinetic, and gravitational potential segmental energy. Note $\frac{d}{dt} E_m$ is computationally equivalent to $P_{JC,m}$ from equation 9 because the vector $-\vec{r}_{COP,m}$ will cancel with the summed vectors $-\vec{r}_{p,m}$, $\vec{r}_{d-AR,m}$, $\vec{r}_{m/m-1}$ and, $\vec{r}_{COP,m-1}$ using the properties of cross and dot products.

$$\frac{d}{dt} E_m = (I_m \vec{\alpha}_m + \vec{\omega}_m \times I_m \vec{\omega}_m) \cdot \vec{\omega}_m + m_m \vec{a}_m \cdot \vec{v}_m - m_m \vec{g} \cdot \vec{v}_m \quad (10)$$

EXPERIMENTAL METHOD

Experimental data were derived from a coded database of nine healthy subjects (34 ± 10 years, 1.69 ± 0.10 m, 75.6 ± 16.2 kg), consented under an IRB approved protocol, walking with

standard shoes on an instrumented treadmill (Bertec Corp., Columbus, OH). Kinematic data were collected using a seven-camera motion capture system (Motion Analysis, Santa Rosa, CA).

Motion capture and force data were sampled at 240 Hz and 1200 Hz and low-pass filtered at 6 Hz and 25 Hz, respectively, and analyzed in Visual3D software (C-Motion, Inc. Germantown, MD). Reflective markers were placed on subjects using a modification to a previously reported marker configuration (Holden et al., 1997). Subjects walked at a height-scaled speed of 0.8 statures/s (approximately 1.4 m/s).

A minimum of 10 strides for the pelvis, left thigh, and left shank were analyzed. In the AR definition, the distal end of a segment was defined in the static model pose and tracked using marker clusters. In the JC definition, the location of the joint center, was determined on a frame-by-frame basis. All power terms were averaged across all subjects and scaled by body mass. Pelvis segmental power was the sum of powers at the left and right hip as well as the proximal pelvis. For each subject, the PI was calculated as the difference between the kinematic method and the kinetic method using the AR definition ($PI_{AR,m}$) or the JC definition ($PI_{JC,m}$) on a frame-by-frame basis across the gait cycle. Maximum and minimum PI were calculated along with the mean PI over the gait cycle for each subject and overall. Mean absolute PI was defined by the absolute value of the PI frame-by-frame averaged across the gait cycle. Mean absolute relative displacement power for the left and right hips are quantified in Supplementary Table 1.

RESULTS

The experimental segmental powers (Fig. 2) and PI (Figs. 3 and 4) revealed $P_{m/m-1}$ accounted for nearly all $PI_{AR,m}$. The average absolute segmental PI was reduced from 0.046 ± 0.015 W/kg, 0.034 ± 0.008 W/kg, and 0.023 ± 0.015 W/kg for the shank, thigh and pelvis,

respectively, using the anatomical definition to $\leq 0.001 \pm 0.000$ W/kg using the joint center definition in the kinetic method. For context, the percent difference between these two measures was 98.4%, 95.7%, and 95.6% for the shank, thigh, and pelvis, respectively.

DISCUSSION

The mathematical analysis presented explains how the segmental PI between segmental power and rate of energy change is influenced by the definition of the distal translational velocity term. An AR definition of the distal translational velocity ignores the relative displacement of segment ends at a joint, resulting in a PI. A JC definition includes a relative displacement power ($P_{m/m-1}$) to accurately equate segmental power and rate of energy change mathematically.

The $P_{m/m-1}$ term computationally accounts for the $PI_{AR,m}$. The addition of the displacement vector $\vec{r}_{m/m-1}$ represents the magnitude of separation at the joint. The cross product of $\vec{\omega}_m$ and $\vec{r}_{m/m-1}$ is a result of relative motion physics (similar in concept to the previously derived distal foot velocity (Siegel et al., 1996)) which represents the relative translational velocity due to the separation of segment ends of the joint. While $P_{m/m-1}$ is included in the m^{th} segment because of our joint center definition, it is a result of imperfect modeling of the instantaneous joint center using marker based motion capture techniques.

Figures 3 and 4 show the magnitude of $P_{m/m-1}$ – previously referred to as an “energy well” (McGibbon and Krebs, 1998) – is substantial. Interestingly, the pelvis had the lowest mean absolute PI. Supplementary Table 1 supports the possibility that relative displacement power at the left and right hips negate each other at parts of the gait cycle. 6 DOF joint power calculations use the JC definition of distal translational velocity (eq. 6), which inherently include the $P_{m/m-1}$ as originally intended when presented by Buczek and colleagues (Buczek et al.,

1994). For explicit clarity, the 6 DOF joint powers include a change in velocity vector (Δv_{joint}) which denotes the difference in segment end velocities at the coincident location of the joint center (Buczek et al., 1994).

Irrespective of whether $\vec{r}_{m/m-1}$ is due to measurement artefact or physiological separation between segment ends at a joint, the translational velocity terms are a necessary inclusion for joint power calculations using 6 DOF models. If the source of $\vec{r}_{m/m-1}$ is due to measurement artefact (e.g. soft tissue movement), then $\vec{r}_{m/m-1}$ will affect segmental angular velocities used to calculate rotational powers. Thus, the true joint power is not better estimated by rotational terms alone. In fact, the results show $P_{m/m-1}$ would be equivalent to the $PI_{AR,m}$ if the primary source of error was joint displacement artefact. Furthermore, if $\vec{r}_{m/m-1}$ is physiological (rather than artefactual), then the same conclusion is reached – translational velocity terms in 6 DOF joint power calculations should not be disregarded.

Although the JC definition for the kinetic method theoretically equates the kinetic and kinematic methods, there remains a small (≤ 0.001 W/kg) average absolute experimental PI. All measures derived from motion and force data are estimates that contribute to errors not shared equally between the kinetic and kinematic methods. Regarding the tracking of motion data, errors may arise from accessory motion of skin-mounted markers due to soft tissue movement making segment endpoints inaccurate (violating rigid body assumptions) and missing axes of rotation (McGibbon and Krebs, 1998; van Ingen Schenau and Cavanagh, 1999; Zajac et al., 2002; Zelik et al., 2015). Regarding the measurement of force data, errors may arise from locating the center of pressure or from estimating the inertial properties of the segments. Furthermore, there may be numerical processing errors due to filtering of motion and force data. Noise in kinematic data due to a series of differentiations or estimates of segment position using

least square calculations of retroreflective marker locations may all be factors for why a PI may be detected experimentally.

A limitation of the 6 DOF model is that traditional motion capture systems cannot precisely measure instantaneous joint translations from surface markers, which would be necessary to fully interpret $P_{m/m-1}$. Note that positive or negative powers at segment ends using the kinetic method produce computationally equivalent segmental energy values based on an assumed uniarticular muscle model to models using biarticular muscles. However, the net power does not identify the source of power generated or absorbed by uni- or biarticular muscles (Kautz et al., 1994; Prilutsky and Zatsiorsky, 1994; van Ingen Schenau and Cavanagh, 1999).

This study shows (1) the relative displacement power ($P_{m/m-1}$) mathematically accounts for the PI between the AR kinetic method and the kinematic method, and (2) the magnitude of $P_{m/m-1}$ is substantial. When tracking power and energy flow between the segments, it is important that the definition of the distal translational velocity is explicitly clear. In conclusion, $P_{m/m-1}$ must be included for the kinetic and kinematic analyses of segmental power to agree. These results support using both rotational and translational power terms to calculate joint powers for 6 DOF models.

CONFLICT OF INTEREST STATEMENT

The authors have no financial or personal relationships with individuals or organizations that inappropriately influenced this work. All authors have no conflicts of interest to disclose.

ACKNOWLEDGEMENTS

This material was based upon work supported by the National Science Foundation (NSF) Graduate Research Fellowship Grant No. 1247394, the Center for Research in Human Movement Variability of the University of Nebraska at Omaha and the National Institute of Health (P20GM109090), the University of Delaware College of Health Sciences, and the Mechanical Engineering Department Helwig Fellowship. It was also supported by the BADER consortium, a Department of Defense Congressionally Directed Medical Research Programs cooperative agreement (W81XWH-11-2-022). The views expressed do not necessarily reflect those of the Department of the Navy, Department of Defense or U.S. Government. Any opinions, findings, and conclusions or recommendations expressed in this material are those of the authors and do not necessarily reflect the views of the NSF.

REFERENCES

- Aleshinsky, S.Y., 1986. An energy “sources” and “fractions” approach to the mechanical energy expenditure problem--V. The mechanical energy expenditure reduction during motion of the multi-link system. *J. Biomech.* 19, 311–315.
- Buczek, F.L., Kepple, T.M., Siegel, K.L., Stanhope, S.J., 1994. Translational and rotational joint power terms in a six degree-of-freedom model of the normal ankle complex. *J. Biomech.* 27, 1447–1457.
- Caldwell, G., Forrester, L., 1992. Estimates of mechanical work and energy transfers: demonstration of a rigid body power model of the recovery leg in gait. *Med. Sci. Sports Exerc.* 24, 1396–1412.
- De Looze, M.P., Bussman, J.B.J., Kingma, I., Toussaint, H.M., 1992. Different methods to estimate total power and its components during lifting. *J. Biomech.* 25, 1089–1095.

- Geil, M.D., Parnianpour, M., Quesada, P., Berme, N., Simon, S., 2000. Comparison of methods for the calculation of energy storage and return in a dynamic elastic response prosthesis. *J. Biomech.* 33, 1745–1750.
- Guo, L.Y., Su, F.C., Wu, H.W., An, K.N., 2003. Mechanical energy and power flow of the upper extremity in manual wheelchair propulsion. *Clin. Biomech.* 18, 106–114.
- Holden, J., Chou, G., Stanhope, S., 1997. Changes in knee joint function over a wide range of walking speeds. *Clin. Biomech.* 12, 375–382.
- Kautz, S.A., Neptune, R.R., 2002. Biomechanical determinants of pedaling energetics: internal and external work are not independent. *Exerc. Sport Sci. Rev.* 30, 159–165.
- Kautz, S., Hull, M., Neptune, R., 1994. A comparison of muscular mechanical energy expenditure and internal work in cycling. *J. Biomech.* 27, 1459–1467.
- McGibbon, C., Krebs, D., 1998. The influence of segment endpoint kinematics on segmental power calculations. *Gait Posture* 7, 237–242.
- Prilutsky, B.I., Zatsiorsky, V.M., 1994. Tendon action of two-joint muscles: transfer of mechanical energy between joints during jumping, landing, and running. *J. Biomech.* 27, 25–34.
- Robertson, D.G.E., Caldwell, G.E., Hamill, J., Kamen, G., Whittlesey, S.N., 2013. *Research Methods in Biomechanics*, 2nd ed, Human Kinetics. Chapter 7.
- Robertson, D.G.E., Winter, D., 1980. Mechanical energy generation, absorption and transfer amongst segments during walking. *J. Biomech.* 13, 845–854.
- Siegel, K., Kepple, T., Caldwell, G., 1996. Improved agreement of foot segmental power and rate of energy change during gait: inclusion of distal power terms and use of three-dimensional models. *J. Biomech.* 29, 823–827.

- Siegler, S., Liu, W., 1997. Inverse Dynamics in Human Locomotion. In: Allard, P., Cappozzo, A., Lundberg, A., Vaughan, C.L. (Eds.), Three-Dimensional Analysis of Human Locomotion. Wiley, New York, 191–209.
- van Ingen Schenau, G., Cavanagh, P.R., 1999. Power equations in endurance sports. *J. Biomech.* 23, 865–881.
- Zajac, F.E., Neptune, R.R., Kautz, S.A., 2002. Biomechanics and muscle coordination of human walking. Part I: introduction to concepts, power transfer, dynamics and simulations. *Gait Posture* 16, 215–232.
- Zelik, K.E., Takahashi, K.Z., Sawicki, G.S., 2015. Six degree-of-freedom analysis of hip, knee, ankle and foot provides updated understanding of biomechanical work during human walking. *J. Exp. Biol.* 218, 876–886.

APPENDIX

Equation 8a in the text can be parsed into two components based on the powers calculated from joint intersegmental forces proximally (Ia) and distally (Ib).

$$\text{Ia. } \vec{F}_{p,m} \cdot \vec{v}_{p,m} = ([\sum_{n=1}^m (m_n \vec{a}_n - m_n \vec{g})] - \vec{F}_{grf}) \cdot (\vec{v}_m + \vec{\omega}_m \times \vec{r}_{p,m})$$

$$= [\sum_{n=1}^m (m_n \vec{a}_n - m_n \vec{g})] \cdot \vec{v}_m - \vec{F}_{grf} \cdot \vec{v}_m$$

$$+ [\sum_{n=1}^m (m_n \vec{a}_n - m_n \vec{g})] \cdot (\vec{\omega}_m \times \vec{r}_{p,m}) - \vec{F}_{grf} \cdot (\vec{\omega}_m \times \vec{r}_{p,m})$$

$$\text{Ib. } \vec{F}_{d,m} \cdot \vec{v}_{d-JC,m} = -([\sum_{n=1}^{m-1} (m_n \vec{a}_n - m_n \vec{g})] - \vec{F}_{grf}) \cdot (\vec{v}_m + \vec{\omega}_m \times \vec{r}_{d-AR,m} + \vec{\omega}_m \times \vec{r}_{m/m-1})$$

$$\begin{aligned}
 &= -[\sum_{n=1}^{m-1} (m_n \vec{a}_n - m_n \vec{g})] \cdot \vec{v}_m + \vec{F}_{grf} \cdot \vec{v}_m \\
 &\quad - [\sum_{n=1}^{m-1} (m_n \vec{a}_n - m_n \vec{g})] \cdot (\vec{\omega}_m \times \vec{r}_{d-AR,m}) + \vec{F}_{grf} \cdot (\vec{\omega}_m \times \vec{r}_{d-AR,m}) \\
 &\quad - [\sum_{n=1}^{m-1} (m_n \vec{a}_n - m_n \vec{g})] \cdot (\vec{\omega}_m \times \vec{r}_{m/m-1}) + \vec{F}_{grf} \cdot (\vec{\omega}_m \times \vec{r}_{m/m-1})
 \end{aligned}$$

The summation of Ia and Ib can be simplified to the following (note the terms **bolded** will be noteworthy later):

$$\begin{aligned}
 \text{Ic. } &\vec{F}_{p,m} \cdot \vec{v}_{p,m} + \vec{F}_{d,m} \cdot \vec{v}_{d-JC,m} \\
 &= (m_m \vec{a}_m - m_m \vec{g}) \cdot \vec{v}_m \\
 &\quad + [\sum_{n=1}^m (m_n \vec{a}_n - m_n \vec{g})] \cdot (\vec{\omega}_m \times \vec{r}_{p,m}) - [\sum_{n=1}^{m-1} (m_n \vec{a}_n - m_n \vec{g})] \cdot (\vec{\omega}_m \\
 &\quad \times \vec{r}_{d-AR,m}) - [\sum_{n=1}^{m-1} (m_n \vec{a}_n - m_n \vec{g})] \cdot (\vec{\omega}_m \times \vec{r}_{m/m-1}) \\
 &\quad - \vec{F}_{grf} \cdot (\vec{\omega}_m \times \vec{r}_{p,m}) + \vec{F}_{grf} \cdot (\vec{\omega}_m \times \vec{r}_{d-AR,m}) + \vec{F}_{grf} \cdot (\vec{\omega}_m \times \vec{r}_{m/m-1})
 \end{aligned}$$

Similarly, equation 8a in the text can be parsed into two components based on powers calculated from net joint moments proximally (IIa) and distally (IIb).

$$\begin{aligned}
 \text{IIa. } &\vec{M}_{p,m} \cdot \vec{\omega}_m \\
 &= [[\sum_{n=1}^m (I_n \vec{a}_n + \vec{\omega}_n \times I_n \vec{\omega}_n + \vec{r}_{COM,n/m} \times (m_n \vec{a}_n - m_n \vec{g}))] - \vec{\tau}_{free} \\
 &\quad - \vec{r}_{COP,m} \times \vec{F}_{grf}] \cdot \vec{\omega}_m
 \end{aligned}$$

$$\text{IIb. } \vec{M}_{d,m} \cdot \vec{\omega}_m$$

$$= -\left[\left[\sum_{n=1}^{m-1} (I_n \vec{a}_n + \vec{\omega}_n \times I_n \vec{\omega}_n + \vec{r}_{COM,n/m-1} \times (m_n \vec{a}_n - m_n \vec{g})) \right] - \vec{\tau}_{free} \right. \\ \left. - \vec{r}_{COP,m-1} \times \vec{F}_{grf} \right] \cdot \vec{\omega}_m$$

The summation of IIa and IIb can be simplified to the following (note the terms **bolded** will be noteworthy later):

$$\text{IIc. } \vec{M}_{p,m} \cdot \vec{\omega}_m + \vec{M}_{d,m} \cdot \vec{\omega}_m$$

$$= (I_m \vec{a}_m + \vec{\omega}_m \times I_m \vec{\omega}_m) \cdot \vec{\omega}_m + \left[\sum_{n=1}^m (\vec{r}_{COM,n/m} \times (\mathbf{m}_n \vec{a}_n - \mathbf{m}_n \vec{g})) \right] \cdot \vec{\omega}_m \\ - \left[\sum_{n=1}^{m-1} (\vec{r}_{COM,n/m-1} \times (\mathbf{m}_n \vec{a}_n - \mathbf{m}_n \vec{g})) \right] \cdot \vec{\omega}_m \\ - (\vec{r}_{COP,m} \times \vec{F}_{grf}) \cdot \vec{\omega}_m + (\vec{r}_{COP,m-1} \times \vec{F}_{grf}) \cdot \vec{\omega}_m$$

Now, considering the terms bolded in IIc, $\vec{r}_{COM,n/m}$ terms for each summation can be expanded.

Here, some terms in these two summations will cancel such that the result of summing IId and IIe will be IIc.

$$\text{IId. } \left[\sum_{n=1}^m (\vec{r}_{COM,n/m} \times (m_n \vec{a}_n - m_n \vec{g})) \right] \cdot \vec{\omega}_m$$

where....

$$\vec{r}_{COM,m/m} = -\vec{r}_{p,m}$$

$$\vec{r}_{COM,m-1/m} = -\vec{r}_{p,m} + \vec{r}_{d-AR,m} + \vec{r}_{m/m-1} - \vec{r}_{p,m-1}$$

$$\vec{r}_{COM,m-2/m} = -\vec{r}_{p,m} + \vec{r}_{d-AR,m} + \vec{r}_{m/m-1} - \vec{r}_{p,m-1} + \vec{r}_{d-AR,m-1} + \vec{r}_{m-1/m-2} - \vec{r}_{p,m-2}$$

etc.

$$\text{Ile. } -[\sum_{n=1}^{m-1}(\vec{r}_{COM,n/m-1} \times (m_n \vec{a}_n - m_n \vec{g}))] \cdot \vec{\omega}_m$$

where....

$$\vec{r}_{COM,m-1/m-1} = -\vec{r}_{p,m-1}$$

$$\vec{r}_{COM,m-2/m-1} = -\vec{r}_{p,m-1} + \vec{r}_{d-AR,m-1} + \vec{r}_{m-1/m-2} - \vec{r}_{p,m-2}$$

$$\text{IIf. } [\sum_{n=1}^m(\vec{r}_{COM,n/m} \times (m_n \vec{a}_n - m_n \vec{g}))] \cdot \vec{\omega}_m$$

$$\begin{aligned} & -[\sum_{n=1}^{m-1}(\vec{r}_{COM,n/m-1} \times (m_n \vec{a}_n - m_n \vec{g}))] \cdot \vec{\omega}_m \\ & = [-\vec{r}_{p,m} \times \sum_{n=1}^m (m_n \vec{a}_n - m_n \vec{g})] \cdot \vec{\omega}_m + [\vec{r}_{d-AR,m} \times \sum_{n=1}^{m-1} (m_n \vec{a}_n - m_n \vec{g})] \cdot \vec{\omega}_m + [\vec{r}_{m/m-1} \\ & \quad \times \sum_{n=1}^{m-1} (m_n \vec{a}_n - m_n \vec{g})] \cdot \vec{\omega}_m \\ & = -1 * [[\sum_{n=1}^m (m_n \vec{a}_n - m_n \vec{g})] \cdot (\vec{\omega}_m \times \vec{r}_{p,m}) - [\sum_{n=1}^{m-1} (m_n \vec{a}_n - m_n \vec{g})] \cdot (\vec{\omega}_m \times \vec{r}_{d-AR,m}) \\ & \quad - [\sum_{n=1}^{m-1} (m_n \vec{a}_n - m_n \vec{g})] \cdot (\vec{\omega}_m \times \vec{r}_{m/m-1})] \end{aligned}$$

Rearranging the terms in IIf and using the properties of cross products, the result is actually the inverse of the bolded term in Ic. Thus, the summation of Ic and IIf will result in equation 9 in the text.

NOMENCLATURE

m_m	segment mass
\vec{a}_m	segment center of mass acceleration

\vec{g}	gravity
\vec{F}_{grf}	ground reaction force
$\vec{F}_{p,m}$	proximal joint intersegmental force
$\vec{F}_{d,m}$	distal joint intersegmental force
$\vec{M}_{p,m}$	proximal net joint moment
$\vec{M}_{d,m}$	distal net joint moment
\vec{I}_m	segment moment of inertia
$\vec{\alpha}_m$	segment angular acceleration
$\vec{\omega}_m$	segment angular velocity
$\vec{\tau}_{free}$	free moment
$\vec{r}_{COM,n/m}$	position vector from proximal segment m to the center of mass of segment n
$\vec{r}_{COP,m}$	position vector from the proximal segment m to the center of pressure
$\vec{v}_{p,m}$	proximal segment velocity
$\vec{r}_{p,m}$	position vector from the center of mass to the proximal segment end
$\vec{r}_{d-AR,m}$	position vector from the center of mass to the anatomically relevant distal segment end
$\vec{r}_{d-JC,m}$	position vector from the center of mass to the joint center (defined as the proximal end of the adjacent distal segment)
$\vec{r}_{m/m-1}$	relative displacement vector between the distal end of segment m and proximal end of segment $m-1$
$\vec{v}_{d-AR,m}$	distal segment translational velocity from the anatomically relevant definition of $\vec{r}_{d-AR,m}$
$\vec{v}_{d-JC,m}$	distal segment translational velocity from the joint center definition of $\vec{r}_{d-JC,m}$
$\vec{v}_{m/m-1}$	relative displacement velocity associated with $\vec{r}_{m/m-1}$
\vec{v}_m	segment center of mass velocity
$P_{AR,m}$	segmental power using the anatomically relevant definition of $\vec{v}_{d-AR,m}$ using kinetic method

$P_{JC,m}$	segmental power using the joint center definition of $\vec{v}_{d-JC,m}$ using kinetic method
$\frac{d}{dt} E_m$	segment rate of energy change using kinematic method
$PI_{AR,m}$	power imbalance between $\frac{d}{dt} E_m$ and $P_{AR,m}$
$PI_{JC,m}$	power imbalance between $\frac{d}{dt} E_m$ and $P_{JC,m}$
$P_{m/m-1}$	relative displacement power term between adjacent segments m and $m-1$
$ PI_{AR,m} _{\text{mean}}$	mean absolute value of the $PI_{AR,m}$
$ P_{m/m-1} _{\text{mean}}$	mean absolute value of the relative displacement power term

Figure Legends

Figure 1: Visual representation of vectors used in inverse dynamics calculations for a 6 DOF multi-segment model. Here, segment m is numbered 1, 2, 3, and 4 which can represent the foot, shank, thigh, and pelvis, respectively. The model shows position vectors from a segment center of mass to the proximal segment end ($\vec{r}_{p,m}$) as well as to the distal segment end using the anatomically relevant (AR) definition ($\vec{r}_{d-AR,m}$) or the joint center (JC) definition ($\vec{r}_{d-JC,m}$). The displacement vector ($\vec{r}_{m/m-1}$) is defined from the AR distal end of the proximal segment m relative to the proximal end of the distal segment $m-1$ (i.e. joint center). Note that all segments are modelled equally, and representations being different on the two limbs are for clarity only. For the pelvis, the displacement vector is from the right or left hip joint center in the pelvis coordinate system (as defined by the static model pose) to the proximal end of the respective thigh. Inset shows notation for the position vectors $\vec{r}_{COM,n/m}$ and $\vec{r}_{COP,m}$ from the proximal segment end to the center of mass of the n^{th} segment (where n is less than or equal to m) and to the center of pressure, respectively.

Figure 2: A noticeable power imbalance exists between segmental power using the anatomically relevant kinetic method ($P_{AR,m}$) and the rate of energy change using the kinematic method ($\frac{d}{dt}E_m$) over 100% of the gait cycle for a representative subject (where m represents the pelvis, left thigh, or left shank). The power imbalance is reduced between the segmental power using the joint center kinetic method ($P_{JC,m}$) and $\frac{d}{dt}E_m$. The power imbalance during swing phase (indicated to the right of the vertical black line at 64.3%) is much smaller than in stance phase due in part to the relatively small power during this phase where there is no ground reaction force.

Figure 3: Average power imbalance between the segmental rate of energy change and the anatomically relevant kinetic method ($PI_{AR,m}$) is almost completely explained by the average power due to the relative segment endpoint displacement ($P_{m/m-1}$), as seen graphed over 100% of the gait cycle (where m represents the pelvis, left thigh, or left shank). Average (± 1 standard deviation in yellow) power imbalance between the segmental rate of energy change and the joint center kinetic method ($PI_{JC,m}$) is relatively small in comparison to $PI_{AR,m}$. The range of $P_{m/m-1}$ is smaller in swing phase (indicated to the right of the vertical black line at 63%) than in stance phase for all three segments, and largest in the left shank compared to the thigh and pelvis over stance phase.

Figure 4: The mean (± 1 standard deviation error bars) absolute power imbalance between the segmental rate of energy change and the anatomically relevant kinetic method ($|PI_{AR,m}|_{\text{mean}}$) averaged across a minimum of 10 gait cycles for each subject shows the inter-subject variability. Overall $|PI_{AR,m}|_{\text{mean}}$ across all subjects (indicated by the blue horizontal line) was 0.046 ± 0.015 W/kg, 0.034 ± 0.008 W/kg, and 0.023 ± 0.015 W/kg for the shank, thigh, and pelvis, respectively. The mean $PI_{AR,m}$ (bracketed numbers under subject data) further highlight the inter-subject variability, revealing no clear pattern in sign or magnitude of mean power imbalance across subjects.

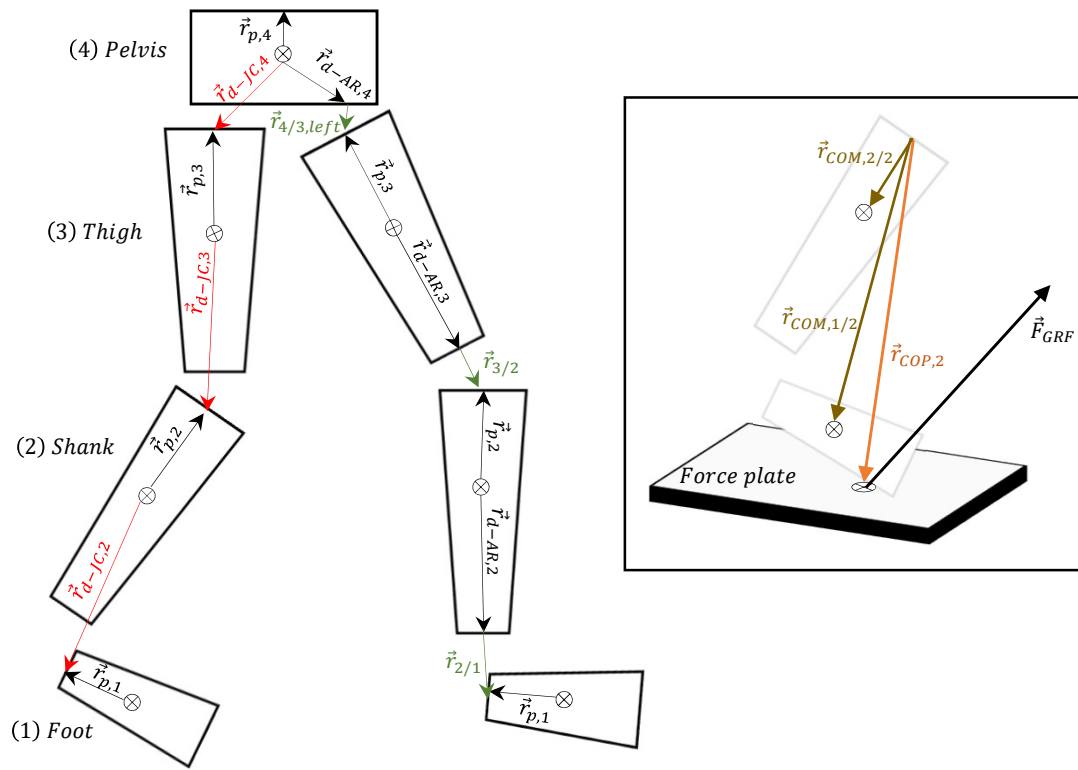


Figure 1.

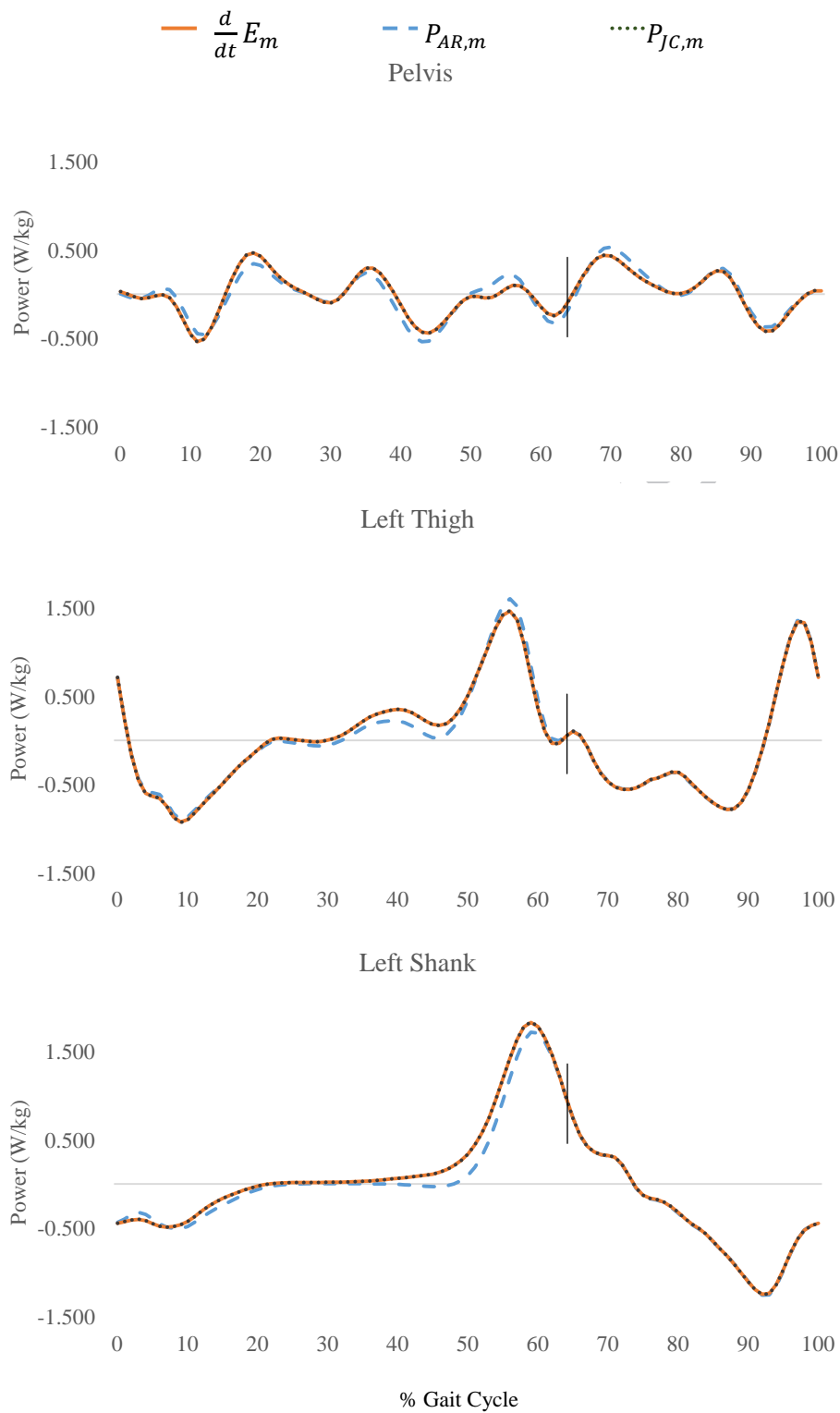
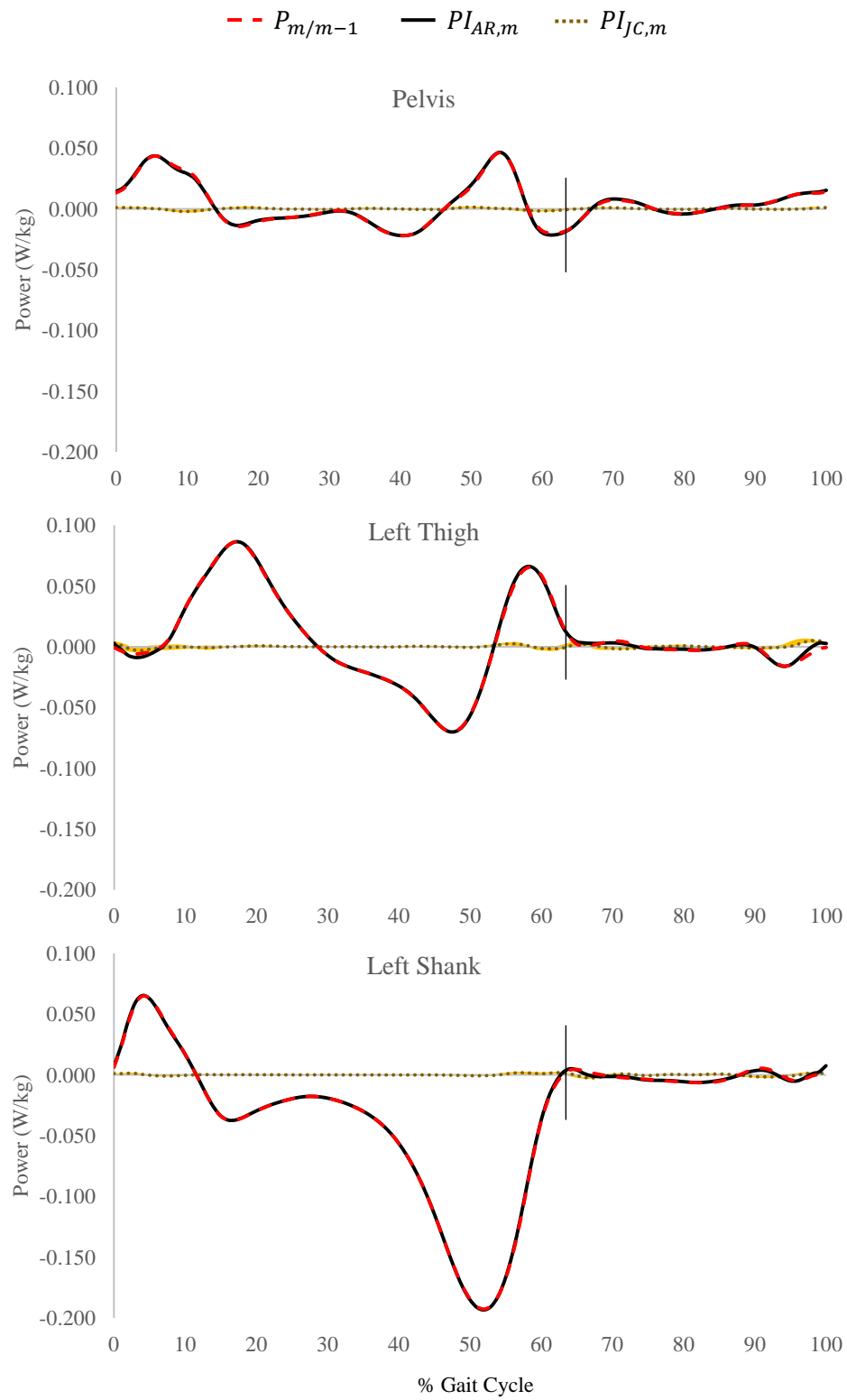


Figure 2.

**Figure 3.**

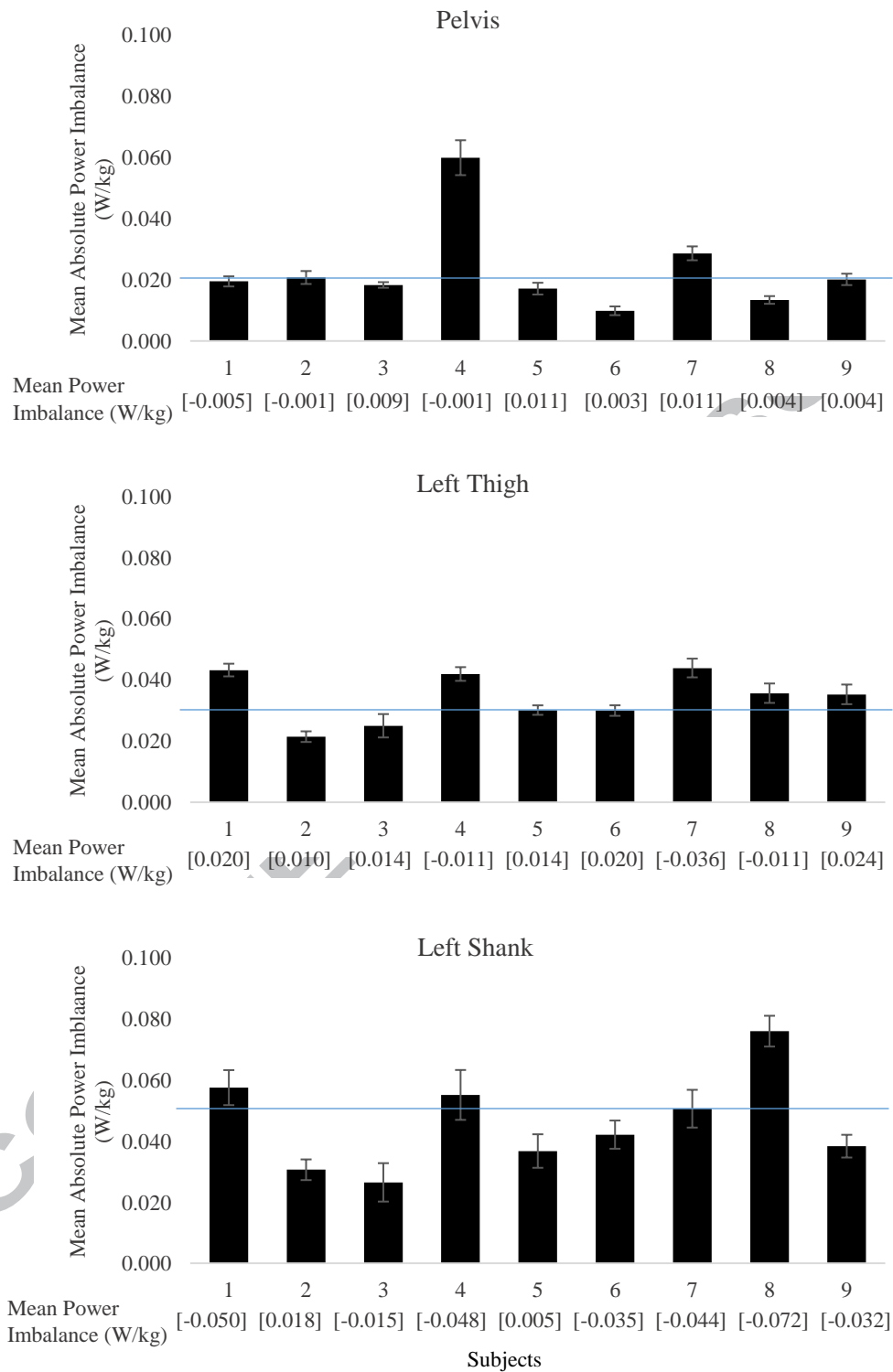


Figure 4.